High Level-of-Detail BIM and Machine Learning for Automated Masonry Wall Defect Surveying

E. Valero[a], A. Forster[a], F. Bosché[a], C. Renier[a], E. Hyslop[b], L. Wilson[b]

[a]Institute for Sustainable Building Design, Heriot-Watt University, Edinburgh EH14 4AS, United Kingdom
[b]Historic Environment Scotland, Salisbury Place, Longmore House, Edinburgh EH9 1SH, United Kingdom
E-mail: {e.valero,a.m.forster,f.n.bosche,cr52}@hw.ac.uk, {ewan.hyslop, lyn.wilson}@hes.scot

Abstract –
Despite the rapid development of reality capture technologies and progress in data processing techniques, current visual strategies for defect surveying are time consuming manual procedures. These methods often deliver subjective and inaccurate outcomes, leading to inconsistent conclusions for defect classification and ultimately repair needs. In this paper, a strategy for monitoring the evolution of ashlar masonry walls of historic buildings through reality capture, data processing (including machine learning), and (H)BIM models is presented. The proposed method has been tested, at different levels of granularity, in the main façade of the Chapel Royal in Stirling Castle (Scotland), demonstrating its potential.

Keywords –
Terrestrial Laser Scanning; Data Processing; Surveying; HBIM; Ashlar

1   Introduction

Whilst traditional approaches to defect identification and analysis are widely utilised, their results have been empirically shown to frequently yield subjective results and mis-classification [1][2]. Attempts to enhance accuracy have been sought in the use of unifying standards and the creation of a 'common language' for the classification of masonry defects [3]. The difficulties faced by surveyors in meaningfully attempting to accurately and rapidly identify defects make the process extremely time-consuming and therefore problematic when 'upscaling' the survey operations from individual masonry units, within localised regions, to complete façades and ultimately entire buildings. On a more fundamental level, the inability of traditional survey to facilitate the labelling of individual masonry units is of significant concern. Yet, all analysis and intervention flow from accurate initial identification of individual materials and components [4]. Indeed, best practice guidance in the conservation sector [5] proposes that those undertaking visual survey and evaluation of historic masonry fabric adopt detailed pictures of the defective areas that can be supplemented by additional information such as measured dimensional survey and a rudimentary process of manually 'marking up' the images with alternative colours denoting different defects. When seen from the perspective of time, cost, accuracy and reproducibility/transferability, these proceses are increasingly untenable.

More recently, novel reality capture technologies, such as Terrestrial Laser Scanning (TLS) or photogrammetry, deliver coloured dense point clouds which can be used to support surveying activities, such as the identification and semantic labelling of the structural and non structural components. Regarding the digitisation of historic buildings, examples of the use of laser scanners include the work of Wilson et al. [6] which illustrates the potential of this technology with several UNESCO heritage sites.

Beyond the sole recording of buildings and other constructions, the unstructured point clouds produced by these devices can also be used for the generation, and subsequent management, of semantically rich digital representation of buildings [7].

In addition to reality capture technology, Building Information Modelling (BIM) is an effective digital approach to the whole lifecycle management of buildings. Besides new construction, for which BIM is used from the conception stage, BIM can be also applied to historic buildings, where it can play a particularly important role in operational maintenance and repair activities. BIM applied to the specific context of historic buildings has become increasingly accepted as HBIM [8][9].

Pronounced differences are noted between BIM and HBIM insomuch that in new projects designs are digitally conceived by means of BIM and CAD design tools, while BIM models of historic buildings need to be produced to reflect their existing (i.e. 'as-is') state, increasingly using dense point clouds as a reference. Hichri et al. [7] provide a general review of the stages to be undertaken from point cloud to BIM, in a process now commonly termed Scan-to-BIM. Similarly, Macher et al. [8] present an approach

to create 3D models of historical buildings by means of point clouds. The authors divide the building in sub-spaces, model surfaces and fit primitive shapes to architectural elements.

The semantically-rich 3D models produced through Scan-to-BIM processes can subsequently be used as a reference to monitor the effects of deterioration. More specifically, decay or change of primary architectural elements or secondary components, such as walls, roofs, etc., can be tracked by means of the processing of newly acquired 3D coloured point clouds and their comparison with the previous known state of the building recorded in the BIM model, using Scan-vs-BIM processes [10].

1.1 Increasing the Level of Detail (LoD) in Scan-to-(H)BIM

Various researchers and practitioners are introducing HBIM to surveys, taking advantage of the structured digital representations of buildings provided by these models [11] [12]. Dore et al. [13] undertook a Scan-to-BIM process for sections of the Four Courts in Dublin and structural damage and decay simulations were applied for conservation analysis. In addition, Oreni et al [14], presented a case study in which HBIM models were generated for digitally surveying an earthquake affected church prior to restoration. This work is particularly interesting in highlighting their approach to the management and evaluation of ashlar columns, whose blocks are individually modelled and their dimensions considered for potential replacement operations.

However, BIM elements, such as walls, typically obtained with these Scan-to-HBIM approaches, do not contain the granularity of composition that is necessary for a detailed annotation and analysis of typical surveys, or require significant manual work to obtain such level of detail. Indeed, surveys may require delineating wall façade defects as effecting a single stone, a cluster of stones (or wall region), or even a part of a stone. There is thus a need for Scan-to-BIM approaches that can efficiently deliver 'as-is' semantically-rich 3D models with such higher LoD – in the case of stone walls, down to the individual stones (and mortar regions).

With the objective of automating these segmentation processes, several authors have recently proposed solutions for the computerised segmentation of images [15] or 3D data [16] of various building elements to support the identification of defective regions. Oses et al. [15] present a semi-automatic process for delineating ashlar in masonry walls in 2D images. Whereas Drap et al. [16] identify clusters of ashlar stones in 3D data. Even if these works propose solutions for dividing structural elements (i.e. walls) into smaller parts, an automated stone-level segmentation process would produce higher LoD representations of walls. Valero et al. [17] previously proposed a method for the automatic

segmentation of random rubble from point clouds. However, whilst it is recognised as a significant step forward, that approach is not well suited to ashlar wall constructions for which 3D data alone may not be sufficient to robustly segment the wall data (mortar depth profiles are often too well aligned with stone profiles to easily detect the stone boundaries using this information alone).

1.2 Survey Objectivity

Whilst defects are wide ranging, they have been codified into five primary categories in the 'ICOMOS glossary of stone deterioration patterns' [3]. These include: Crack and deformation; Detachment; Features induced by material loss; Discolouration and deposit; and, finally, Biological colonisation. These are the broad categories that have been adopted for this research.

The heterogeneity and sophistication of these catalogued defects make their labelling process complex, even for professionals, who can differ in their analysis. For example, historic building walls are composed of hundreds, and in many instances thousands, of unique units (i.e. stones, bricks…), and can be affected by almost countless defects. Sánchez et al [18] proposed a novel strategy to identify, in point clouds, the deformation and erosion of walls and highlight unit clusters (i.e. areas) affected by decay. Valero et al. [4] have recently proposed the use of geometric and colour-related features from individual masonry units relevant to interpretation or conservation purposes, but that interpretation remained manual.

While these recent works investigate the potential of using point clouds to detect wall defects, these remain preliminary in nature. They do not fully automate defect detection and classification, or do this in a limited way, both in terms of the range of defects being detectable and the depth of the classification/analysis.

1.3 Contribution

This paper aims to address the two needs identified at the end of the previous two sub-sections. We first present a novel Scan-to-(H)BIM approach that automatically segments point clouds of ashlar masonry walls into their constitutive units, i.e. stones, and mortar regions (Section 2). Then, we propose a novel machine learning based approach to masonry wall defect classification, that considers both the geometry and colour information of the acquired point clouds, to classify a selective range of common types of masony wall defects (Section 3). The defects are found in relation to the masonry HBIM element and constitutive units, and so can be recorded in a structured manner within the HBIM model, so that the condition of all architectural components can be effectively tracked over time.

For the theoretical presentation of those two novel contributions, Section 4 reports experimental results obtained using real data. Finally, Section 5 concludes the works and proposes directions of future research development.

2 High LoD HBIM Masonry Wall Element

In this work, principal building elements, such as roof or walls, are referred to as *elements*, that can be subsequently segmented into their constitutive sub-elements, named *units*. These would include bricks or stones in the case of walls (See Figure 1). Furthermore, if several contiguous units are affected by the same defects, these should be recorded and studied as a region. Therefore, we refer to several adjoining units composing regions of interest as *clusters*. Finally, certain defects can affect only parts of a unit. We call such region a *sub-unit* region.
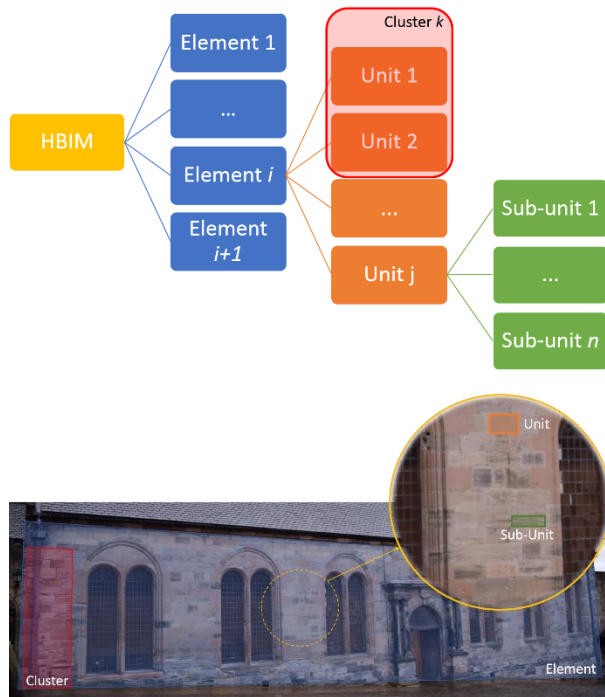

Figure 1. Proposed levels for analysis. Ilustration for a wall.

To deliver the hierarchical subdivision described above, a segmentation process was developed to identify the individual masonry units composing the overall element. This method considers colour and 3D information at both local and global level and it is grounded on the analysis of data in the frequency domain.

The 2D Continuous Wavelet Transform (CWT) is applied to identify the joints between units and segment individual stones (see Figure 2).
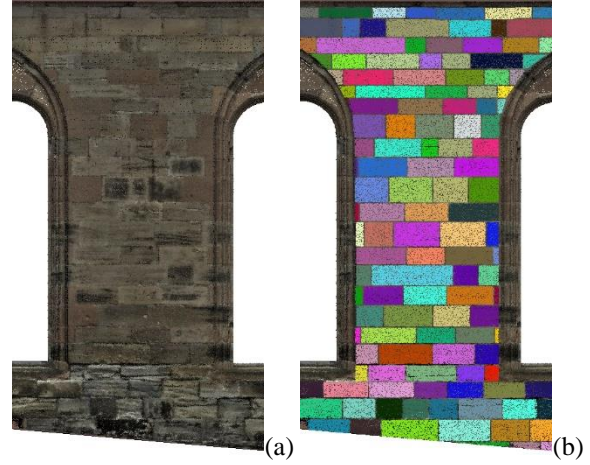

Figure 2. Ashlar masonry wall. (a) Coloured point cloud. (b) Segmented ashlar units.

3 Identification of Defects using Machine Learning

Several geometric and colour metrics are presented in this section, that highlight stone regions potentially affected by decay, at different levels, both unit and sub-unit (Section 3.1). These are used for defects classification by means of machine learning (Section 3.2).

3.1 Metrics for the Identification of Defects

Once units are segmented and labelled, information regarding geometry and colour is extracted from each stone and several parameters are calculated to evaluate its state.

In the case of coursed ashlar, two specific parameters can play an important role to identify decayed units. Regarding geometric-based defects, the evaluation of the roughness of the stone face profile helps differentiate between flat and rough masonry units. Higher levels of roughness can suggest stones affected by deformation and detachment, related in most cases with loss of material. Roughness is calculated as the standard deviation of the distance of the profile points to the profile's mean plane:

$$Ra = \sqrt{\frac{1}{N}\sum_{i=1}^{N}(d_i - \mu)^2}, \text{ with } \mu = \frac{1}{N}\sum_{i=1}^{N} d_i \quad (1)$$

where N is the number of 3D points for the given stone face and d_i's are the projection distances of those points to the fitted plane.

With respect to colour-related defective areas, the analysis of the dispersion of colour in each stone, by means of the calculation of the standard deviation of the hue values within each ashlar unit (Equation (2)), can be used to highlight zones affected by discolouration or other defects associated to color, such as efflorescence or biological colonisation.

$$H_\sigma = \sqrt{\frac{1}{N}\sum_{i=1}^{N}(h_i - \mu)^2}, \text{ with } \mu = \frac{1}{N}\sum_{i=1}^{N}h_i \qquad (2)$$

for which the Red-Green-Blue (RGB) colour data is first converted into Hue-Saturation-Value (HSV) format, using the algorithm presented in [19].

The evaluation of these two parameters can be undertaken at the unit level (i.e. stone), resulting in the generation of two colour maps as illustrated in Figure 3. Figure 3 (a) corresponds to the roughness map, while Figure 3(b) illustrates stones potentially affected by defects related to colour variation. Traffic light colour maps have been used, in which the stones coloured in green are less likely to be affected by decay and the yellow and red ones are potentially defective.
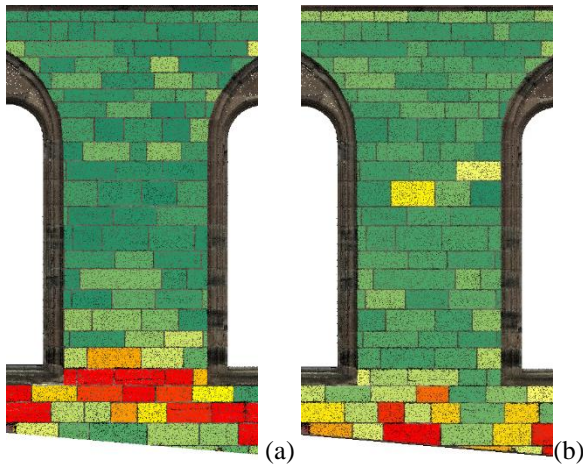

Figure 3. Geometry- and colour-based parameters. (a) Ra. (b) H_σ.

These above parameters and subsequently produced maps are of value for unit-level analysis and are useful to highlight clusters affected by decay. However, a more detailed analysis (i.e. at sub-stone scale) can deliver information about the precise defects which are affecting a specific stone.

The fine dressing of ashlar masonry, especially in polished finishes, facilitates the detection of defective areas. In these cases, the stone profile should fit a plane, with areas potentially affected by geometry-related defects can be found as those containing the outliers. Figure 4 illustrates, for each ashlar, the inliers (in green)

and the outliers, which are coloured from yellow to red, according to the distance of the recorded 3D points to the fitted plane. Regions coloured in red are those with a more pronounced loss of material.

Figure 4. Sub-stone level analysis map.

3.2 Machine Learning Approach for Defects Classification

An extended evaluation of the areas containing outliers can be undertaken in order to identify the particular effects affecting the material. Figure 5 (a) illustrates a decayed region of ashlar, where a plane is fitted to the stone and the outliers are considered to be part of a defective area (see darker points in Figure 5 (b)). While 3D coordinates are used to calculate the roughness coefficient (the point cloud is coloured according to their depth in Figure 5 (c)), additional metrics are calculated after the binary image obtained from the 3D point outliers (see Figure 5 (d)).
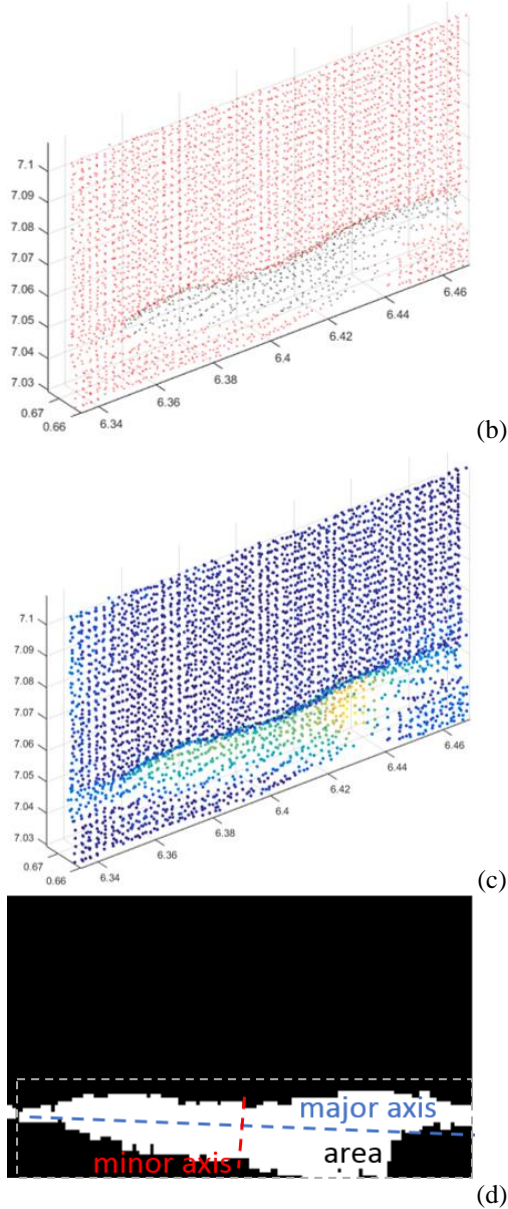

(a)

(b)

(c)

(d)
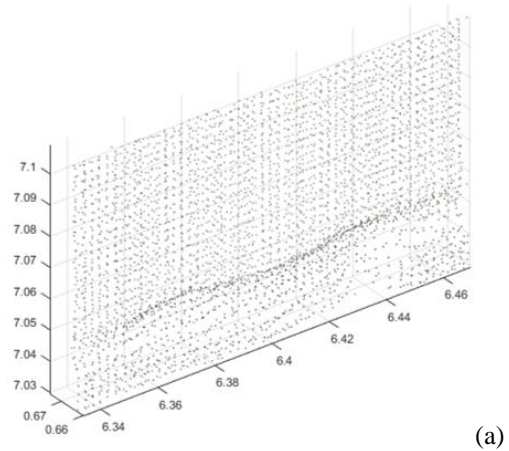
Figure 5. Process for parameters extraction. (a) Original coloured point cloud (b) Inliers (red) and outliers (gray) after plane fitting (c) Depth map for outliers (d) Binary map created after orthogonal projection of outliers.

From the 3D coordinates of the outliers, two metrics are extracted:

- Ra, the roughness coefficient of the defective area, (Equation (1)), and
- The median value of the normal vectors of the outliers with respect to the plane fitting the ashlar.

From the binary map obtained after the projection of the ouliers, the following parameters are considered:

- the number and area of unconnected defective areas (white segments in Figure 5(d)),
- the elongation of the defective areas, which is the ratio of the lengths of the minor to major axes and gives an indication of how 'oblong' a defective area is,
- the rectangleness of the defective areas, which is calculated as the fraction of the bounding box covered by the object, and
- the circularity of the defective areas, which is the ratio of the area of the projection of the defective region to the area of a circle with the same perimeter (p), as detailed in Equation (3).

$$C = \frac{4 \cdot area \cdot \pi}{p^2} \qquad (3)$$

From the colour information of the points associated to the defective area, two metrics are extracted:

- H_σ , as detailed in Equation (2).
- Colour lightness. RGB colour data are converted to grayscale [20], and the median value of g_i, (the grayscale value of each point inside the defective area) is calculated to provide information about the colour lightness.

Machine learning techniques are effective tools for classification and analysis. In this work, we propose a supervised learning algorithm to classify masonry units affected by different types of decay, and using the parameters described above. Stones labelled as 'defective' by professional surveyors, as illustrated in Figure 6, are used for training the classifier and producing an inferred function that is subsequently employed to automatically label new data.
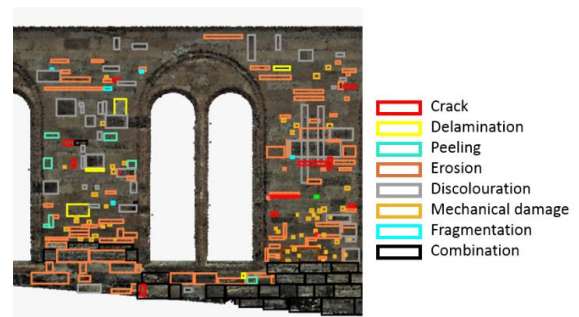

Figure 6. Defective areas labelled by surveyors.

The chosen machine learning algorithm may vary depending on the number and nature of samples in the studied dataset and features [21]. In this work, after evaluating the amount of available samples and the extracted features, a logistic regression algorithm has been employed.

4   Experimental Results

The proposed approach has been tested with data from the main façade of the Royal Chapel in Stirling Castle, Scotland. A coloured dense point cloud (see Figure 7) has been produced after merging four scans acquired with a Leica P40 TLS device [22].

4.1   HBIM and Unit-level Maps

The generated point cloud was considered as a reference to create an 'as-is' 3D model of the Chapel Royal's façade. This model, that distinguishes the wall, door and windows (Figure 8) is used as the base of an HBIM model.

After removing the points corresponding to the door and the windows using a Scan-vs-BIM process, the point cloud composing the wall is segmented, producing a database with 1,116 ashlar units, as illustrated in Figure 9.

The points assigned to each ashlar unit are then automatically processed to calculate the parameters mentioned in the Subsection 3.1. Two maps, containing the values of Ra and H_σ can be seen in Figure 10.

As can be observed in Figure 10, the bottom part of the façade is found to be potentially affected by both geometry and colour-related defects. Also, the left and right ends of the walls have decayed regions. Physical inspection of the wall confirmed long term deterioration associated with previously defective rain water downcomers, leading to higher fabric moisture contents and subsequent increased incidence of freeze thaw decay processes. In addition, the presence of white 'blooms' were noted and are most likely attributed to salt crystallisation.

Figure 7. Dense coloured point cloud of Chapel Royal's main façade.

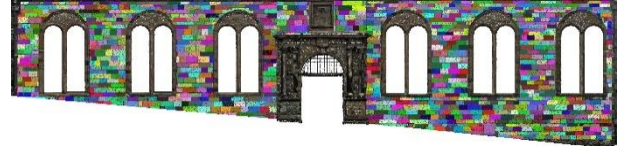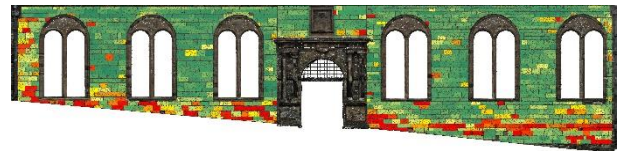Figure 8. Rendered 3D model of the façade.

Figure 9. Segmented ashlar units

(a)

(b)

Figure 10. Colourmaps generated for the façade. (a) Roughness. (b) Standard deviation of hue values.

All produced outcomes in the form of colourmaps, were subsequently added to the HBIM model (see Figure 11) adding information that can be contrasted with the status of the structural components at previous epochs.
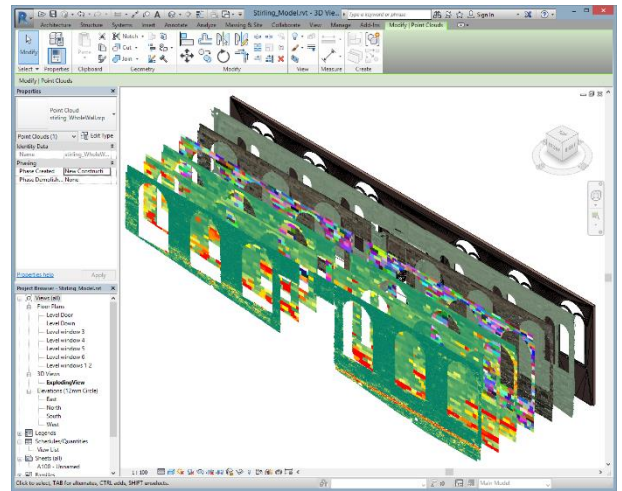

Figure 11. Datasets attached to the HBIM model.

4.2   Classification of Labelled Defective Areas

To enhance the rapidity, accuracy and objectivity of labelling, machine learning techniques were developed and applied. The initial classification (i.e. labelling) of defective stones and broader areas was performed by

specialist surveyors with expertise in masonry fabric repair and deterioration. The Stirling Castle Royal Chapel's ashlar façade was used and comprehensively surveyed and subsequently adopted to test the algorithms.

As previously illustrated in Figure 6, approximately 230 defective stone areas were labelled by specialist surveyors. Although approximately ten different types of defects were identified, only three of them were representative in significant numbers to be considered in this study: erosion (E), mechanical damage (M) and discolouration (D). The frequency of those most repeated defects is detailed in Table 1.

Table 1 Frequency of defects identified by surveyors in the studied area

Defect	Repetitions
Erosion	77
Mechanical damage	53
Discolouration	43

As previously mentioned in Section 3.2, the logistic regression algorithm was then employed, performing a 'one vs all' training process. For the training process, random samples of these three classes (72 from erosion, 48 labelled as mechanical damage and 38 identified as discolouration), were used as input to the algorithm. A maximum of 50 iterations has been used, with a regularization parameter applied to the cost function.

A total of 15 samples (5 of each class) were included in the test set, obtaining a global accuracy of 93.3% in the classification. More detailed results are summarized in Table 2. Additionally, Table 3 shows recall and precision values for the classification process.

Table 2 Confusion matrix for the classification of defects

	E	M	D	Predicted
E	4	0	0	4
M	0	5	0	5
D	1	0	5	6
Labelled	5	5	5	15

Table 3 Precision and recall values for the different classes

	Recall	Precision
Erosion	0.8	1
Mechanical	1	1
Discolouration	1	0.83

5   Conclusions

A strategy for monitoring the evolution of ashlar masonry walls of historic buildings through reality capture, data processing including machine learning, and (H)BIM models is presented in this paper. Different levels of magnitude are considered to perform surveying tasks: from element to sub-unit levels, several point clouds and maps are produced to illustrate the defective regions of the studied façades. At a sub-stone level, a more detailed analysis is carried out to extract different metrics which are of interest to identify decayed areas by means of machine learning techniques.

A preliminary experiment has been performed with geospatial data from a historic building and the obtained results demonstrate the potential of the proposed methodology.

References

[1] Forster, A. M. and Douglas, J. Condition survey objectivity and philosophy driven masonry repair: An increased probability for project divergence? *Structural Survey*, 28 (5), pages 384-407, 2010. https://doi.org/10.1108/02630801011089173.

[2] Straub, A. Dutch standard for condition assessment of buildings. *Structural Survey*, 27 (1), pages 23-35, 2009. https://doi.org/10.1108/02630800910941665.

[3] ICOMOS. International Scientific Committee for Stone. *ICOMOS-ISCS: Illustrated Glossary on Stone Deterioration Patterns*. ICOMOS, Paris, 2008.

[4] Valero, E., Bosché, F., Forster, A. and Hyslop, E. Historic Digital Survey: Reality Capture and Automatic Data Processing for the Interpretation and Analysis of Historic Architectural Rubble Masonry. *Manuscript submitted for publication*, 2018.

[5] Urquhart, D. *Stonemasonry skills and materials: A methodology to survey sandtone building facades. Technical Advice Note number 31*. Historic Scotland, Edinburgh, 2007.

[6] Wilson, L., Rawlinson, A., Mitchell, D., McGregor, H. and Parsons, R. .The Scottish Ten Project: Collaborative Heritage Documentation. In *XXIV International CIPA Symposium*, pages 685–690, Strasbourg, France, 2013.

[7] Hichri, N., Stefani, C., De Luca, L., Veron, P. and Hamon, G. From Point Cloud to BIM: A Survey of

Existing Approaches. In *International Archives of the Photogrammetry, Remote Sensing and Spatial Information Sciences,* XL-5/W2, 2013 XXIV International CIPA Symposium, pages 343–348, Strasbourg, France, 2013. http://doi.org/10.5194/isprsarchives-XL-5-W2-343-2013.

[8] Macher, M., Landes, T., Grussenmeyer, P. and Alby, E. Semi-automatic Segmentation and Modelling from Point Clouds towards Historical Building Information Modelling. In Marinos Ioannides, Nadia Magnenat-Thalmann, Eleanor Fink, Roko Žarnic, Alex-Yianing Yen, and Ewald Quak, editors, *Digital Heritage. Progress in Cultural Heritage: Documentation, Preservation, and Protection*, volume 8740 of *Lecture Notes in Computer Science*, pages 111–120. Springer International Publishing, 2014. https://doi.org/10.1007/978-3-319-13695-0_11.

[9] Historic England. BIM for Heritage: Developing a Historic Building Information Model. Historic England, Swindon, United Kingdom, 2017. Online: https://content.historicengland.org.uk/images-books/publications/bim-for-heritage/heag-154-bim-for-heritage.pdf/. Accessed: 17/01/2018.

[10] Bosché, F., Guillemet, A., Turkan, Y. and Haas, C.T. Tracking the Built Status of MEP Works: Assessing the Value of a Scan-vs-BIM System. *Journal of Computing in Civil Engineering*, 28(4), 2013. https://doi.org/10.1061/(ASCE)CP.1943-5487.000034.

[11] Brumana, R., Oreni, D., Raimondi, A., Georgopoulos, A. and Bregianni, A. From survey to HBIM for documentation, dissemination and management of built heritage: The case study of St. Maria in Scaria d'Intelvi. In *2013 Digital Heritage International Congress (DigitalHeritage)*, pages 497-504. Marseille, France, 2013. http://doi.org/10.1109/DigitalHeritage.2013.6743789.

[12] Oreni, D., Brumana, R., Georgopoulos, A. and Cuca, B. HBIM for Conservation and Management of Built Heritage: Towards a Library of Vaults and Wooden Bean Floors. *ISPRS Annals of Photogrammetry, Remote Sensing and Spatial Information Sciences,* II-5/W1: 215 – 221, 2013. http://doi.org/10.5194/isprsannals-II-5-W1-215-2013.

[13] Dore, C., Murphy, M., McCarthy, S., Brechin, F., Casidy, C. and Dirix, E. Structural Simulations and Conservation Analysis - Historic Building Information Model (HBIM). *ISPRS - International Archives of the Photogrammetry, Remote Sensing and Spatial Information Sciences*, XL-5/W4, 351-357, 2015. http://doi.org/10.5194/isprsarchives-XL-5-W4-351-2015.

[14] Oreni, D., Brumana, R., Della Torre, S., Banfi, F., Barazzetti, L. and Previtali, M. Survey turned into HBIM: the restoration and the work involved concerning the Basilica di Collemaggio after the earthquake (L'Aquila). *ISPRS Annals of Photogrammetry, Remote Sensing and Spatial Information Sciences*, II-5, 267-273, 2014. http://doi.org/10.5194/isprsannals-II-5-267-2014.

[15] Oses, N. and Dornaika, F. Image-Based Delineation of Built Heritage Masonry for Automatic Classification. In Mohamed Kamel and Aurélio Campilho, editors, *Image Analysis and Recognition, volume 7950 of Lecture Notes in Computer Science*, pages 782–789. Springer Berlin Heidelberg, 2013.

[16] Drap, P., Merad, D., Boi, J., Seinturier, J., Peloso, D., Reidinger, C., Vannini, G., Nucciotti, M. and Pruno, E. Photogrammetry for Medieval Archaeology: A Way to Represent and Analyse Stratigraphy. In *Proceedings of 18th International Conference on Virtual Systems and Multimedia (VSMM)*, pages 157–164, Milan, Italy, September 2012. http://doi.org/10.1109/VSMM.2012.6365920.

[17] Valero, E., Bosché, F. and Forster, A. Automatic Segmentation of 3D Point Clouds of Rubble Masonry Walls, and its Application to Building Surveying, Repair and Maintenance. *Mansucript submitted for publication*, 2018.

[18] Sánchez-Aparicio, L. J., Del Pozo, S., Ramos, L. F., Arce, A. and Fernandes, F. M. Heritage site preservation with combined radiometric and geometric analysis of TLS data. *Automation in Construction*, 85, 24-39, 2018, https://doi.org/10.1016/j.autcon.2017.09.023.

[19] Smith A. R. Color Gamut Transform Pairs. In *Proceedings of SIGGRAPH 78 Conference*, pages 12-19. New York, August, 1978. https://doi.org/10.1145/965139.807361.

[20] Anderson M., Motta R., Chandrasekar S. et Stokes, M. Proposal for a Standard Default Color Space for the Internet—sRGB. In *4th Color and Imaging Conference Proceedings*, pages 238-245(8), United States, 1996.

[21] Mohri, M., Rostamizadeh, A. and Talwalkar, A. *Foundations of Machine Learning*. The MIT Press, Cambridge, Massachusetts, 2012.

[22] Leica Geosystems. Leica ScanStation P30/P40. Online: https://leica-geosystems.com/products/laser-scanners/scanners/leica-scanstation-p40--p30. Accessed: 10/01/2018.